

VIPHY: Probing “Visible” Physical Commonsense Knowledge

Shikhar Singh, Ehsan Qasemi, Muhao Chen

University of Southern California

Los Angeles, California, USA

{ssingh43, qasemi, muhaoche}@usc.edu

Abstract

In recent years, vision-language models (VLMs) have shown remarkable performance on visual reasoning tasks (e.g. attributes, location). While such tasks measure the requisite knowledge to ground and reason over a given visual instance, they do not, however, measure the ability of VLMs to retain and generalize such knowledge. In this work, we evaluate their ability to acquire “visible” physical knowledge – the information that is easily accessible from images of static scenes, particularly across the dimensions of object color, size and space. We build an automatic pipeline to derive a comprehensive knowledge resource for calibrating and probing these models. Our results indicate a severe gap between model and human performance across all three tasks. Furthermore, our caption pretrained baseline (CapBERT) significantly outperforms VLMs on both size and spatial tasks – highlighting that despite sufficient access to ground language with visual modality, they struggle to retain such knowledge. The dataset and code are available at <https://github.com/Axe--/ViPhy>.

1 Introduction

The ability to reason and acquire knowledge from experience, while being intuitive for humans, has been a long-standing challenge for AI agents (McCarthy et al., 1960). Examples such as the color of grass, or the relative position of monitor and table, are formally regarded as commonsense knowledge (Chi, 2005). The retention of such knowledge in humans is achievable due to the presence of long-term memory, broadly classified into *episodic* and *semantic* memory (Tulving, 1972; Camina and Güell, 2017). While the former stores information pertaining to personal events, the latter is geared towards general, decontextualized knowledge.¹ Prior

¹For instance, memory of one’s birthday cake is episodic, whereas knowing that most birthdays include a cake is part of semantic memory.

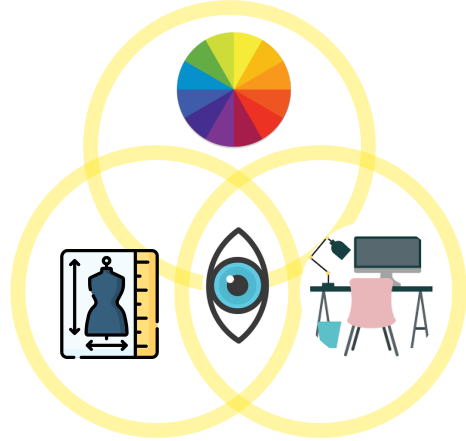


Figure 1: We propose VIPHY – the trinity of visually accessible knowledge representing color, size and space.

studies (Greenberg and Verfaellie, 2010) have acknowledged the interdependency between them, particularly the *consolidation* of semantic knowledge from episodic memories – aids humans acquire commonsense from experience.

Pretrained language models (Devlin et al., 2018; Raffel et al., 2020) have demonstrated the capacity to reason (Wang et al., 2019) and retain knowledge (Petroni et al., 2019; Da et al., 2021). Likewise, vision-language models (Lu et al., 2019; Radford et al., 2021) driven by the availability of large-scale paired image-text datasets have shown strong performance on visual reasoning tasks (Antol et al., 2015; Chen et al., 2015). While such tasks emphasize model’s ability to draw inferences from a specific visual instance – primarily to ground entities and reason about their attributes and relations, they do not, however, explicitly measure the consolidation of such knowledge.² In this work, we evaluate model’s ability to recall aspects of grounding and reasoning tasks, regarded as commonsense

²An example of reasoning is counting bike wheels in an image, whereas knowing that bikes have two wheels is consolidation.

knowledge.

Prior works have been largely directed towards probing language models pertaining to object properties such as weight, size, speed and affordance (Forbes and Choi, 2017; Forbes et al., 2019). Drawing upon the notion of world scopes (Bisk et al., 2020a), we find that such datasets, albeit comprehensive across aspects of physical knowledge, are ideally suited for embodied agents capable of interacting with the physical environment. This motivates us to develop resources that better align with the world scope of existing AI systems, primarily vision-language models.

In this work, we introduce VIPHY, a **visible physical commonsense** dataset designed to probe aspects of physical knowledge that are easily accessible in images of static scenes. Therefore, it can be argued that models pretrained on such data have sufficient access to the “visible world”. We build a large-scale dataset along three dimensions of objects: (1) color, (2) size, and (3) space. In contrast to prior works (Paik et al., 2021), we bypass crowdsourced annotations in favor of an automated pipeline to derive a resource spanning 14k objects (30×) from raw images. This is achieved by extracting object subtypes – informed by visual context in images (e.g. kitchen sink). We leverage image data, along with existing vision-language and depth perception models to develop VIPHY.

Beyond scale, we introduce a resource for probing spatial knowledge of common environments. Albeit, one can reason along several types of spatial relations for a visual instance (e.g. a cat *behind* a laptop; Liu et al. (2022a)) – we find that mapping them to commonsense knowledge is non-trivial³. We define spatial relations by selecting “ground” as the observer, and specifying the relative elevation of objects under an allocentric reference frame (Klatzky, 1998).

We probe state-of-the-art models on VIPHY, and find significant gap across all three dimensions, compared to human performance. Previous works (Paik et al., 2021; Liu et al., 2022b) have corroborated the improvements from language grounding towards acquiring visual knowledge – our results however, show a more nuanced picture. While VLMs fair much better than LMs on recalling colors, our caption pretrained baseline (CapBERT) significantly outperforms VLMs on both size and

³Due to challenges in specifying the reference frame of the observer, canonical pose of the objects, and the situational nature of a scene.

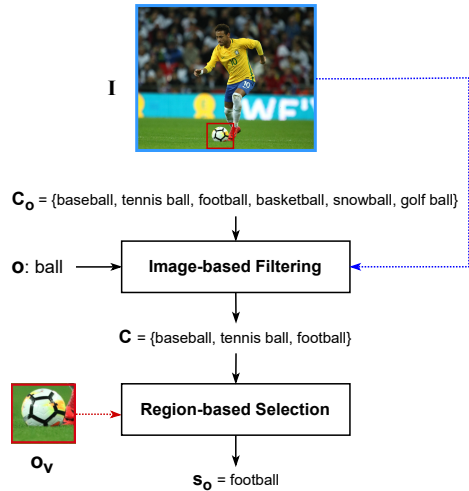


Figure 2: Subtype Selection Module: Given object o in image I , assigns subtype s_o from candidate set C_o .

spatial inference tasks. This highlights that despite access to visual modality, existing VLMs struggle to effectively consolidate such knowledge.

The contributions of this work can be as summarized as follows: (1) We contribute with a comprehensive dataset, covering multiple aspects of visually accessible knowledge (§3), which is introduced through an automated pipeline to derive high-quality resource from images at scale (§2); (2) We conduct extensive benchmarking across several state-of-the-art language and vision-language models (§4); (3) We introduce a caption pretrained baseline that significantly outperforms state-of-the-art VLMs on several dimensions of VIPHY, highlighting of limitations of such models.

2 Pipeline

We provide a conceptual overview of our pipeline for developing VIPHY, as illustrated in Fig. 3. Given image and object regions as input⁴, we substitute object names with their subtypes (§2.1), and compute the corresponding depth map. The subtype candidates are acquired from image captions and knowledge bases. After preprocessing, we independently extract color (§2.2), size (§2.3) and spatial knowledge (§2.4).

2.1 Object Subtype

While object recognition datasets consider a wide range of objects, such tasks do not necessitate fine-grained categories (Zou et al., 2019). However,

⁴Available from either manual annotations or object detection / segmentation model (e.g. He et al. (2017)).

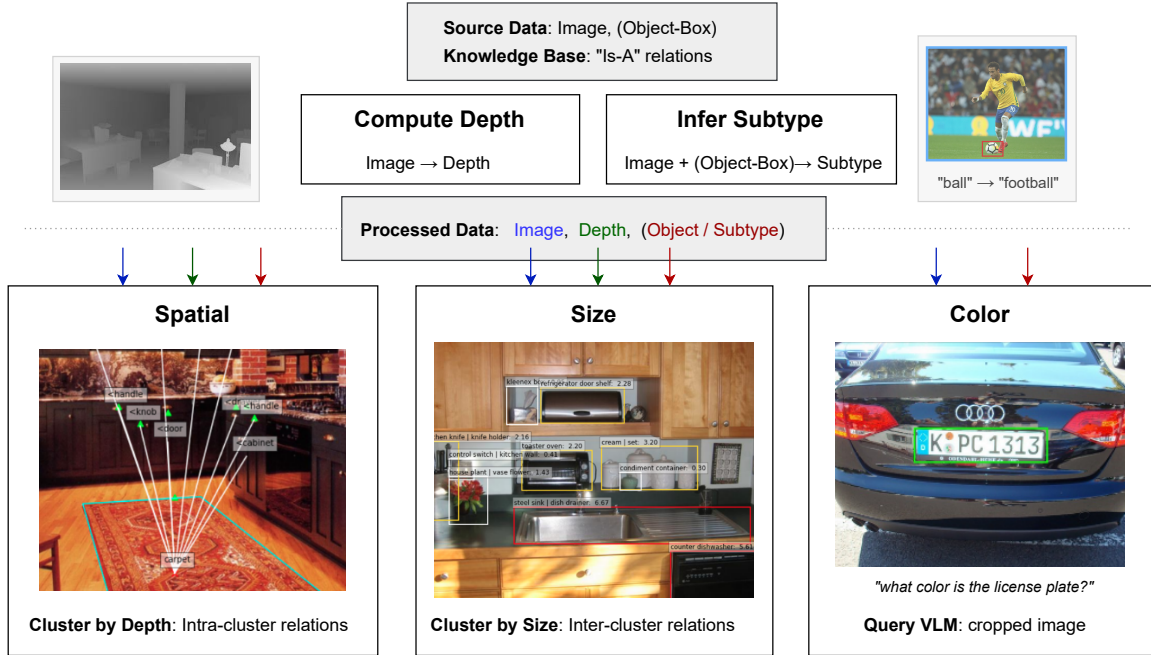


Figure 3: Pipeline Overview: The preprocessing stage computes the depth map for input image and re-annotates object regions with their subtype. It then independently extracts color, size and spatial knowledge.

object *subtypes* inform attributes such as color, and help contextualize objects in absence of visual signals (e.g. office chair). Albeit, subtypes are generally accessible from knowledge bases (KB), their coverage is often limited.⁵ We extend this definition to include objects defined by visual context – indicating event, location, state, part, etc. (Appendix Tab. 8). For **subtype collection**, we parse the captions to build a set of object names. We then employ suffix-based lexical matching to derive subtypes for each object, and merge with hyponyms from knowledge base. The resulting data represents a mapping between the object name and its candidate subtypes.

As our goal is to derive object attributes and relations directly from images, we design a **subtype selection** module to annotate the source image regions with the best subtype. This is required since human annotators often abstract the object name to avoid redundancy when presented with visual context (example in Appendix Fig. 9), congruent with the maxim of quantity (Grice, 1975). Likewise, existing object detectors are not suited for open-vocabulary and fine-grained classification (Minderer et al., 2022).

The module is designed to query from subtype candidates using visual features. It employs a two-

stage approach to filter candidates using image context, and select the best subtype with region-level features, as illustrated in Fig. 2. The visual and textual inputs are embedded using a dual stream vision-language model. Formally, given the visual feature of the image I , textual features of the object o and subtype candidates C_o , we extract the appropriate subtype as follows:

$$C = \{c | c \in C_o, \text{sim}(c, I) > \text{sim}(o, I)\} \cup o$$

Here, $\text{sim}(\cdot)$ is the cosine similarity. Intuitively, since the object name is independent of visual context, it serves as an anchor for excluding subtypes that do not align with the contextual cues. In the next stage, we incorporate visual features of the object region o_v , to query from filtered candidate set C , and compute the best subtype s_o :

$$s_o = \arg \max_{c \in C} \text{sim}(o_v, c)$$

The resulting dataset comprises of object-subtype mapping for bounding box regions in the image.

2.2 Color

Prior works (Paik et al., 2021) have relied on human annotations to acquire the color distribution of objects instead of inferring color from pixel values due to challenges such as lighting, shadow, segmentation, etc. However, we argue that large-scale availability of images can mitigate potential

⁵We report ~60% object name overlap between our collection and ConceptNet KB (Speer et al., 2017).

noise associated with automated extraction. Given the ubiquity of color attribute in visual reasoning tasks (Antol et al., 2015; Hudson and Manning, 2019), we find that VLMs pretrained on such datasets are reliable for inferring color from images. As object localization is decoupled from attribute recognition in the pipeline, the input to the VLM is simply the cropped image region, queried with a predefined textual prompt (detailed in §3.1).

2.3 Size

To derive size relations, we consider co-occurring objects in a scene. As objects in an image are expected to appear at varying depths, we approximate perceived size by including scene depth. Given an image, depth map and object-region annotations as inputs, the objects are clustered by size – defined as the bounding box area scaled by mean depth of the region. The sorted partitions are then used to derive inter-cluster relations. The object pair relations are aggregated across images. The number of clusters are fixed for all instances.

2.4 Spatial

We define spatial knowledge as the relative elevation between objects, for a given scene type. To infer these relations directly from image, however, is challenging as perspective projection of 3D world distorts the relative elevation due to variation in depth. We discount this distortion by partitioning the image by depth, and compute *intra-cluster* object relations, *i.e.* we discard the depth coordinate of objects that belong to the same cluster, and simply compare the relative elevation. The *inter-cluster* relations are derived transitively via overlapping partitions – defined by objects with dual membership, as illustrated in Fig. 4. The spatial relations are aggregated across all images for a given scene type. We detail the specifics of mapping object annotations to spatial relations in Appendix A.3.

3 Dataset

This section details the specific data sources and models used to develop VIPHY, and dataset statistics (§3.2). We also describe the task format (§3.3) for each dimension. Additional parameters related to dataset construction are provided in Appendix A.1.

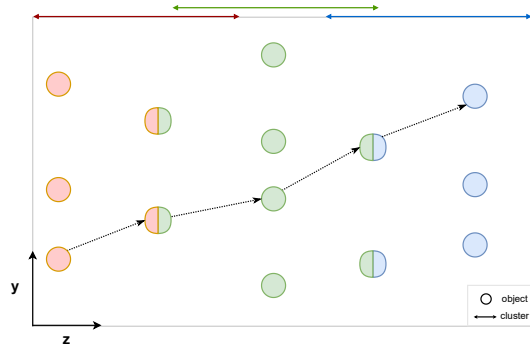


Figure 4: Illustrates transitive spatial relation, computed across partitions (ordered by depth). The y-axis denotes elevation, while the z-axis indicates depth.

3.1 Construction

Sources We leverage two datasets: (1) Visual Genome (Krishna et al., 2017), and (2) ADE20K (Zhou et al., 2017). The dense captions in Visual Genome provide a broad coverage of object classes, making it a suitable resource for collecting subtype candidates. For extracting hyponyms from knowledge base, we acquire "is-a" relations from ConceptNet (Speer et al., 2017), and augment the subtype candidate set. We extract spatial relations from ADE20K, as it provides images categorized by scene type – primarily indoor environments with high object density: $\{bedroom, bathroom, kitchen, living\ room, office\}$.

Models To collect subtype candidates (as detailed in §2.1), we perform part-of-speech tagging to extract object names (noun) from caption data, using LSTM-CRF (Akbik et al., 2018). For subtype selection, we employ UniCL (Yang et al., 2022) – designed for discriminative representations and broad semantic coverage of entities. To compute depth map from monocular image, we use DPT (Ranftl et al., 2021). To infer object color from image region (§2.2), we query OFA (Wang et al., 2022), using the prompt template: “what color is the <object>?”. The zero-shot predictions from OFA are mapped to the basic color set (Berlin and Kay, 1991) as detailed in Appendix A.4.

3.2 Statistics

Table 1 summarizes statistics for VIPHY, comprising the number of objects, classes and instances for each dimension. For multi-label tasks, we report the label cardinality, *i.e.* number of labels for a sample. We also indicate the number of objects with

Subtype	objects	14k
	objects with subtype	1.8k
	subtype cardinality	7.73 (12.91)
Color	objects (instances)	14k
	classes	11
	label cardinality	2.42 (1.37)
Size	objects	1.6k
	instances	43k
	relations	2
Spatial	objects	300
	instances	6.5k
	relations	3
	label cardinality	1.28 (0.45)
	scenes	5

Table 1: Dataset statistics for ViPHY. The cardinality is reported with mean and standard deviation.

subtypes and subtype cardinality⁶. Note that while we extract size relations and color attributes from same source images (§3.1), we ignore *contextual* subtypes for size relations, as they serve a limited role towards informing object size (e.g. rain coat). However, as we only consider co-occurring objects, we implicitly incorporate context for objects in comparison, *i.e.* help disambiguate word sense. We collect 7.1k smaller and 14.5k larger relations, and balance labels by including their complements. The label distributions of color dataset is provided in Appendix Fig. 7.

3.3 Task Setup

The objective of ViPHY tasks is to measure the ability to recall physical knowledge pertaining to objects. To probe models with textual prompts, we map the raw distribution of labels (acquired by our pipeline) to typical values, as detailed in Appendix A.2. In the **color** task, objects can have multiple labels from the set of 11 basic colors as defined in Berlin and Kay (1991): *{red, orange, yellow, brown, green, blue, purple, pink, white, gray, black}*. Likewise, we consider multiple labels for **spatial** relations from *{below, above, similar level}*, conditioned on a scene type as mention in §3.1. Lastly, **size** relations are mapped to a single label from *{smaller, larger}*.

4 Experiments

We evaluate several state-of-the-art models under zero-shot and finetune settings (§4.1), and conduct further analysis of model performance (§4.2). The

⁶Note: The subtype cardinality is only reported for objects with subtype.

datasets are partitioned into 20% train, 10% dev, 70% test set.

Baselines We consider the following language (LM) and vision-language (VLM) models:

- **LMs:** BERT (Devlin et al., 2018), RoBERTa (Liu et al., 2019), DeBERTa (He et al., 2020) and UnifiedQA (Khashabi et al., 2020).
- **VLMs:** VisualBERT (Li et al., 2019), ViLT (Kim et al., 2021), CLIP (Radford et al., 2021) and FLAVA (Singh et al., 2022).

CapBERT In addition to the aforementioned baselines, we explore the following question: To what degree does an LM pretrained only on image captions – encodes visual knowledge. In contrast to the standard corpora which comprises a broad range of knowledge domains, captions primarily describe the visual aspects of the world. We build CapBERT by pretraining BERT_{base} on captions from COCO (Chen et al., 2015), CC3M (Sharma et al., 2018) and VG (Krishna et al., 2017) datasets.

Finetuning To evaluate under finetune setting, we train a linear classifier on top of the model’s output, while rest of the weights are frozen. We use Softmax Cross Entropy loss for single and multi-label setups, following Mahajan et al. (2018). All probes are finetuned for 50 epochs, with batch size of 8, using Adam optimizer (Kingma and Ba, 2014) and a learning rate of 10^{-4} .

Prompts For probing LMs and VLMs, we provide manually designed textual prompt as input to the model. The prompt templates for probing across color, size and spatial tasks, under zero-shot (ZS) and finetune (FT) settings are given in Table 2. Besides models trained on the masked language objective⁷, the question-answering baseline (UnifiedQA) follows a common template⁸ for both ZS and FT settings.

Metrics We introduce the following metrics for measuring task performance under multi-label setting:

- **Relaxed Accuracy (R-Acc)** – The prediction (P) is accurate if the most probable label be-

⁷CLIP being the exception, cannot be evaluated under ZS setting. Under FT, it uses EOS instead of CLS token.

⁸The prompt includes all classes as choices.

Task	Setting	Prompt
Color	ZS	O is of [MASK] color
	FT	[CLS] color of O
	QA	What is the color of O ? (a) .. (b) ..
Size	ZS	O_1 is [MASK] than O_2 in size
	FT	[CLS] size of O_1 in comparison to O_2
	QA	what is the size of O_1 in comparison to O_2 ? (a) .. (b) ..
Spatial	ZS	in a S , the O_1 is located [MASK] the O_2
	FT	[CLS] in a S , the O_1 is located in comparison to O_2
	QA	in a S , where is O_1 is located in comparison to O_2 ? (a) .. (b) ..

Table 2: Prompt templates across tasks and evaluation settings. Here, O , R and S are placeholders for object, relation and scene type respectively.

longs to the ground-truth labels (T).

$$RA = \sum_{i \in D} \frac{[l_i \cap T_i] \wedge [l_i = \arg \max_l P_i(l)]}{|D|}$$

- True Confidence (Conf) – The sum of predicted probabilities for labels in the ground-truth set.

$$C = \sum_{i \in D} \frac{\sum_{l \in T_i} P_i(l)}{|D|}$$

Here, D denotes samples in the evaluation set. In addition to the aforementioned metrics, we also report the macro-averaged F1-score (F1).

Human Performance To provide an upper bound on VIPHY tasks, we use CoDa (Paik et al., 2021) for color – computed over 432 overlapping objects⁹. For size and spatial dataset, we internally evaluate 100 relations with two annotators (authors) and report the average score.

4.1 Results

Zero-Shot We report zero-shot performance using R-Acc metric, across all tasks in Table 3. For spatial task, we only consider two labels from $\{above, below\}$, due to the limitation of single word masking in selected baselines. We observe significant variations in model performance across tasks, with VLMs (VisualBERT) performing worse than their LM counterparts – underscoring the challenges of manual prompting (Jiang et al., 2020). The best scoring baseline (UnifiedQA) falls at least 30% points below human scores.

⁹The label distributions of VIPHY and CoDa are provided in Appendix – Fig. 7 and Fig. 8

Model	Color	Size	Spatial
BERT _{large}	48.39	44.61	20.96
RoBERTa _{large}	0.59	47.01	17.52
UnifiedQA _{large}	51.00	51.76	63.04
VisualBERT	9.06	24.91	9.57
Human	97.45	94.32	95.12

Table 3: Zero-shot results (R-Acc) across all tasks.

Model	R-Acc	Conf	F1
CapBERT	70.45	58.55	40.91
BERT _{base}	66.87	55.59	30.94
RoBERTa _{large}	55.95	49.28	20.93
UnifiedQA _{large}	62.34	-	-
DeBERTa _{xxl}	72.74	59.59	36.33
VisualBERT	66.22	50.99	24.46
ViLT	64.83	53.92	30.27
FLAVA	76.33	62.84	38.74
CLIP	79.96	65.50	49.54
Human _{CoDa}	97.45	78.65	72.12

Table 4: Color results.

Model	R-Acc	Conf	F1
CapBERT	69.93	62.09	60.78
BERT _{base}	67.25	59.91	61.34
RoBERTa _{large}	54.88	58.40	58.88
UnifiedQA _{large}	62.04	-	-
DeBERTa _{xxl}	62.30	61.27	60.54
VisualBERT	63.08	58.40	58.88
ViLT	65.78	60.28	59.80
FLAVA	63.71	61.06	60.56
CLIP	65.10	63.56	62.26
Human	95.12	-	87.42

Table 5: Spatial results.

Finetune When compared to zero-shot results, we report improved calibration under finetuned probing, as evident from results on color (Tab. 4), size (Tab. 6) and spatial tasks (Tab. 5). We find that VLMs score higher than LMs – specifically their “caption-only” counterpart (CapBERT) on the color task. These results hint at the role of color attribute in grounding entities. However, CapBERT outperforms VLMs on both size and spatial tasks, implying that despite having access to visual representations, VLMs do not retain such relational knowledge as effectively. Lastly, CapBERT outperforming other LMs is likely due to the domain similarity between the pretraining source and the evaluation tasks¹⁰.

¹⁰For instance, a prepositional phrase can convey both abstract (*on schedule*) and physical (*on table*) relations, with captions predominantly containing the latter.

Model	Standard	Subtype	Transitive
CapBERT	83.69	79.14	91.82
BERT _{base}	78.35	72.28	77.29
RoBERTa _{large}	65.23	57.12	69.31
UnifiedQA _{large}	62.20	60.66	90.78
DeBERTa _{xxl}	74.73	66.88	69.79
LM_{average}	69.37	64.23	74.54
VisualBERT	76.99	64.00	77.69
ViLT	78.54	57.32	86.18
FLAVA	82.67	69.54	81.78
CLIP	75.43	66.56	72.48
VLM_{average}	79.15	64.35	79.53
Human	94.32	-	-

Table 6: Size results reported across different evaluation sets, measured by accuracy (random baseline: 50%).

4.2 Analysis

Color: Cardinality We further analyze model performance with respect to label cardinality (i.e. number of ground-truth colors for an object), by grouping objects accordingly. As shown in Fig. 5, we report results for three baselines, their average, along with human scores. While the performance is expected to increase with the cardinality¹¹, we notice an inconsistency between model and human scores. In particular, while difference in overall confidence scores (as inferred from Table 4) for human and the model average is ~18%, the relative differences between the two – ranges from ~12% ($x = 6$) to ~40% ($x = 1$), where x -axis denotes the label cardinality. While color influences object perception in humans (Gegenfurtner and Rieger, 2000), these results show that VLMs do not ascribe a similar degree of saliency to color, especially for uni-color objects (i.e. cardinality of one).

Size: Transitivity As the size dataset¹² is composed of frequently co-occurring object pairs, we intend to evaluate models ability to infer relative size for objects linked transitively across scenes. We build a new evaluation set comprising transitive relations from the standard size dataset, ensuring no overlapping instances between the two. The results (Tab. 6) indicate that LMs (on average) improve by significant margin, compared to VLMs. While the improvements on the evaluation set can be partially attributed to objects on the relatively

¹¹R-Acc & Conf are 1, when cardinality is 11.

¹²For reference, the #instances for size evaluation sets are as follows – standard: 30k, subtype: 23k, transitive: 20k.

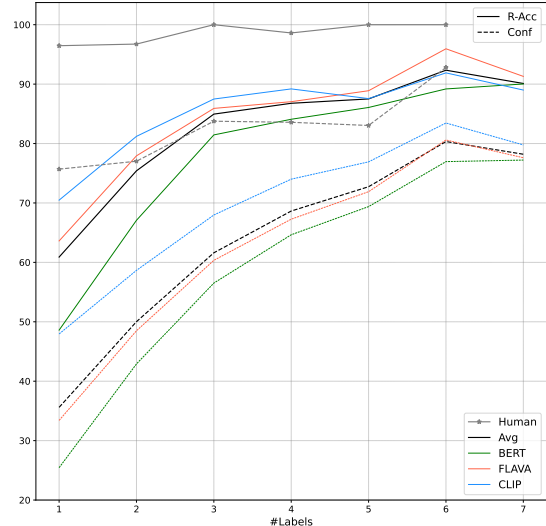


Figure 5: Effect of label cardinality (x -axis) on color prediction, as measured by R-Acc and Conf. The Avg curves (black) indicate average model performance.

extreme ends of size clusters being paired up, they are able to generalize on transitive relations.

Size: Subtypes While contextual qualifiers tend to inform the typicality of color attribute, their effect on size is likely inconsequential. Therefore, models should retain their performance with reference to the standard set. We test this hypothesis by creating an evaluation set comprising contextual subtypes for objects in the standard test set. While the addition of subtypes leads to performance drop across all models (Tab. 6), we find that LMs are more robust in comparison to VLMs.

5 Related Works

Physical Commonsense Recent years have witnessed a renewed interest in studying commonsense, primarily via natural language benchmarks (Talmor et al., 2019; Singh et al., 2021). Specific works have evaluated the language models on their ability to reason about physical commonsense (Bisk et al., 2020b; Qasemi et al., 2022). Others have identified reporting bias as a potential bottleneck for models pretrained on text corpora towards acquiring physical knowledge (Forbes et al., 2019; Paik et al., 2021). In this work, we direct our focus towards vision-language models pretrained on large paired image-text datasets, and evaluate them on visually accessible commonsense knowledge. While prior works have probed knowledge pertaining to color (Paik et al., 2021) and size (Talmor et al., 2020), their coverage of objects is severely limited in comparison to VIPHY (30×).

Recently, Liu et al. (2022a) have comprehensively evaluated spatial reasoning for 65 relation types, given an image and a caption as inputs. In contrast, VIPHY measures the ability to recall spatial commonsense. Additionally, whereas Liu et al. (2022b) have probed spatial knowledge for human-object interaction (224 instances) under 15 action types (e.g. driving, cooking), we consider the spatial layout of objects across scene types over 6k instances, independent of events.

Vision-Language Resources While image classification (Deng et al., 2009) can be construed as one of the earliest attempts at bridging vision and language, recent years have witnessed a plethora of resources. Visual reasoning tasks have been directed towards object attributes (Antol et al., 2015), activities (Chen et al., 2015), as well as social (Zellers et al., 2019) and temporal commonsense (Fu et al., 2022). Recently, VLMs (Lu et al., 2019; Li et al., 2020; Radford et al., 2021) have demonstrated strong performance on such tasks. These works evaluate the requisite knowledge to reason about a specific instance, VIPHY in contrast probes the knowledge retained in the absence of visual context, *i.e.* generalized from instances.

Knowledge in LMs Recent advancements in language models (Devlin et al., 2018; Raffel et al., 2020), pretrained on large corpora, has led to significant improvements across several reasoning tasks (Wang et al., 2019). Prior works have also highlighted the capacity of these models to acquire several types of knowledge such as factual (Petroni et al., 2019; Roberts et al., 2020), instructional (Huang et al., 2022) and commonsense (Da et al., 2021). In this work, we study to what degree do their vision-language analogs (VLMs) – driven by the availability of massive paired image-text datasets, retain information that is easily accessible in images.

6 Conclusion

We present VIPHY, a large scale resource for probing “visible” physical knowledge – information easily accessible from images of static scenes, across dimensions of color, size and space. We design an automated pipeline to extract and consolidate such knowledge facts from images, and introduce a new resource for evaluating spatial knowledge of common environments. Our benchmarking evaluation highlights a huge gap between model and

human performance across all three tasks. Furthermore, while prior works have reported VLMs to be more effective, our caption pretrained baseline (CapBERT) significantly outperforms VLMs on the ability to recall size and spatial knowledge. These results underscore that despite access to visual modality, existing VLMs struggle to retain visual knowledge as effectively.

Ethical Implications

We build VIPHY from existing images from crowd-verified visual datasets which have been identified to lack geographical diversity, often limited to scenes from Europe and North America (Shankar et al., 2017). Furthermore, such datasets are subjected to several kinds of biases at different stages of collection and annotation such as selection bias, framing bias and observer bias (Fabrizzi et al., 2022). Therefore, its likely that such biases will be reflected in our dataset as well. As we also report benchmarking results on VIPHY, the model performance may not be reflected as accurately on knowledge pertaining to different geographical and cultural backgrounds, as studied in Yin et al. (2021). Lastly, our proposed resource is limited to English, and thus excludes any considerations for multilingual models (Yin et al., 2022).

Acknowledgement

This work is supported in part by the DARPA MCS program under Contract No. N660011924033 with the United States Office Of Naval Research.

References

- Alan Akbik, Duncan Blythe, and Roland Vollgraf. 2018. Contextual string embeddings for sequence labeling. In *COLING 2018, 27th International Conference on Computational Linguistics*, pages 1638–1649.
- Stanislaw Antol, Aishwarya Agrawal, Jiasen Lu, Margaret Mitchell, Dhruv Batra, C Lawrence Zitnick, and Devi Parikh. 2015. Vqa: Visual question answering. In *Proceedings of the IEEE international conference on computer vision*, pages 2425–2433.
- Brent Berlin and Paul Kay. 1991. *Basic color terms: Their universality and evolution*. Univ of California Press.
- Yonatan Bisk, Ari Holtzman, Jesse Thomason, Jacob Andreas, Yoshua Bengio, Joyce Chai, Mirella Lapata, Angeliki Lazaridou, Jonathan May, Aleksandr Nisnevich, et al. 2020a. Experience grounds language. In *Proceedings of the 2020 Conference on*

- Empirical Methods in Natural Language Processing (EMNLP)*, pages 8718–8735.
- Yonatan Bisk, Rowan Zellers, Jianfeng Gao, Yejin Choi, et al. 2020b. Piqa: Reasoning about physical commonsense in natural language. In *Proceedings of the AAAI conference on artificial intelligence*, volume 34, pages 7432–7439.
- Eduardo Camina and Francisco Güell. 2017. The neuroanatomical, neurophysiological and psychological basis of memory: Current models and their origins. *Frontiers in pharmacology*, 8:438.
- Xinlei Chen, Hao Fang, Tsung-Yi Lin, Ramakrishna Vedantam, Saurabh Gupta, Piotr Dollár, and C Lawrence Zitnick. 2015. Microsoft coco captions: Data collection and evaluation server. *arXiv preprint arXiv:1504.00325*.
- Micheline TH Chi. 2005. Commonsense conceptions of emergent processes: Why some misconceptions are robust. *The journal of the learning sciences*, 14(2):161–199.
- Jeff Da, Ronan Le Bras, Ximing Lu, Yejin Choi, and Antoine Bosselut. 2021. Analyzing commonsense emergence in few-shot knowledge models. In *3rd Conference on Automated Knowledge Base Construction*.
- Jia Deng, Wei Dong, Richard Socher, Li-Jia Li, Kai Li, and Li Fei-Fei. 2009. Imagenet: A large-scale hierarchical image database. In *2009 IEEE conference on computer vision and pattern recognition*, pages 248–255. Ieee.
- Jacob Devlin, Ming-Wei Chang, Kenton Lee, and Kristina Toutanova. 2018. Bert: Pre-training of deep bidirectional transformers for language understanding. *arXiv preprint arXiv:1810.04805*.
- Simone Fabbrizzi, Symeon Papadopoulos, Eirini Ntoutsi, and Ioannis Kompatsiaris. 2022. A survey on bias in visual datasets. *Computer Vision and Image Understanding*, page 103552.
- Maxwell Forbes and Yejin Choi. 2017. Verb physics: Relative physical knowledge of actions and objects. In *Proceedings of the 55th Annual Meeting of the Association for Computational Linguistics (Volume 1: Long Papers)*, pages 266–276.
- Maxwell Forbes, Ari Holtzman, and Yejin Choi. 2019. Do neural language representations learn physical commonsense? In *CogSci*.
- Xingyu Fu, Ben Zhou, Ishaan Chandratreya, Carl Vondrick, and Dan Roth. 2022. **There’s a time and place for reasoning beyond the image**. In *Proceedings of the 60th Annual Meeting of the Association for Computational Linguistics (Volume 1: Long Papers)*, pages 1138–1149, Dublin, Ireland. Association for Computational Linguistics.
- Karl R Gegenfurtner and Jochem Rieger. 2000. Sensory and cognitive contributions of color to the recognition of natural scenes. *Current Biology*, 10(13):805–808.
- Daniel L Greenberg and Mieke Verfaellie. 2010. Interdependence of episodic and semantic memory: Evidence from neuropsychology. *Journal of the International Neuropsychological society*, 16(5):748–753.
- Herbert P Grice. 1975. Logic and conversation. In *Speech acts*, pages 41–58. Brill.
- Kaiming He, Georgia Gkioxari, Piotr Dollár, and Ross Girshick. 2017. Mask r-cnn. In *Proceedings of the IEEE international conference on computer vision*, pages 2961–2969.
- Pengcheng He, Xiaodong Liu, Jianfeng Gao, and Weizhu Chen. 2020. Deberta: Decoding-enhanced bert with disentangled attention. *arXiv preprint arXiv:2006.03654*.
- Wenlong Huang, Pieter Abbeel, Deepak Pathak, and Igor Mordatch. 2022. Language models as zero-shot planners: Extracting actionable knowledge for embodied agents. *arXiv preprint arXiv:2201.07207*.
- Drew A Hudson and Christopher D Manning. 2019. Gqa: A new dataset for real-world visual reasoning and compositional question answering. In *Proceedings of the IEEE/CVF conference on computer vision and pattern recognition*, pages 6700–6709.
- George F Jenks. 1967. The data model concept in statistical mapping. *International yearbook of cartography*, 7:186–190.
- Zhengbao Jiang, Frank F Xu, Jun Araki, and Graham Neubig. 2020. How can we know what language models know? *Transactions of the Association for Computational Linguistics*, 8:423–438.
- Daniel Khashabi, Sewon Min, Tushar Khot, Ashish Sabharwal, Oyvind Tafjord, Peter Clark, and Hananeh Hajishirzi. 2020. Unifiedqa: Crossing format boundaries with a single qa system. *arXiv preprint arXiv:2005.00700*.
- Wonjae Kim, Bokyung Son, and Ildoo Kim. 2021. Vilt: Vision-and-language transformer without convolution or region supervision. In *International Conference on Machine Learning*, pages 5583–5594. PMLR.
- Diederik P Kingma and Jimmy Ba. 2014. Adam: A method for stochastic optimization. *arXiv preprint arXiv:1412.6980*.
- Roberta L Klatzky. 1998. Allocentric and egocentric spatial representations: Definitions, distinctions, and interconnections. In *Spatial cognition*, pages 1–17. Springer.

- Ranjay Krishna, Yuke Zhu, Oliver Groth, Justin Johnson, Kenji Hata, Joshua Kravitz, Stephanie Chen, Yannis Kalantidis, Li-Jia Li, David A Shamma, et al. 2017. Visual genome: Connecting language and vision using crowdsourced dense image annotations. *International journal of computer vision*, 123(1):32–73.
- Liunian Harold Li, Mark Yatskar, Da Yin, Cho-Jui Hsieh, and Kai-Wei Chang. 2019. Visualbert: A simple and performant baseline for vision and language. *arXiv preprint arXiv:1908.03557*.
- Xiujun Li, Xi Yin, Chunyuan Li, Pengchuan Zhang, Xiaowei Hu, Lei Zhang, Lijuan Wang, Houdong Hu, Li Dong, Furu Wei, et al. 2020. Oscar: Object-semantic aligned pre-training for vision-language tasks. In *European Conference on Computer Vision*, pages 121–137. Springer.
- Fangyu Liu, Guy Emerson, and Nigel Collier. 2022a. Visual spatial reasoning. *arXiv preprint arXiv:2205.00363*.
- Xiao Liu, Da Yin, Yansong Feng, and Dongyan Zhao. 2022b. Things not written in text: Exploring spatial commonsense from visual signals. In *Proceedings of the 60th Annual Meeting of the Association for Computational Linguistics (Volume 1: Long Papers)*, pages 2365–2376.
- Yinhan Liu, Myle Ott, Naman Goyal, Jingfei Du, Mandar Joshi, Danqi Chen, Omer Levy, Mike Lewis, Luke Zettlemoyer, and Veselin Stoyanov. 2019. Roberta: A robustly optimized bert pretraining approach. *arXiv preprint arXiv:1907.11692*.
- Jiasen Lu, Dhruv Batra, Devi Parikh, and Stefan Lee. 2019. Vilbert: Pretraining task-agnostic visiolinguistic representations for vision-and-language tasks. *Advances in neural information processing systems*, 32.
- Dhruv Mahajan, Ross Girshick, Vignesh Ramanathan, Kaiming He, Manohar Paluri, Yixuan Li, Ashwin Bharambe, and Laurens Van Der Maaten. 2018. Exploring the limits of weakly supervised pretraining. In *Proceedings of the European conference on computer vision (ECCV)*, pages 181–196.
- John McCarthy et al. 1960. *Programs with common sense*. RLE and MIT computation center Cambridge, MA, USA.
- Matthias Minderer, Alexey Gritsenko, Austin Stone, Maxim Neumann, Dirk Weissenborn, Alexey Dosovitskiy, Aravindh Mahendran, Anurag Arnab, Mostafa Dehghani, Zhuoran Shen, et al. 2022. Simple open-vocabulary object detection with vision transformers. *arXiv preprint arXiv:2205.06230*.
- Cory Paik, Stéphane Aroca-Ouellette, Alessandro Roncone, and Katharina Kann. 2021. The world of an octopus: How reporting bias influences a language model’s perception of color. In *Proceedings of the 2021 Conference on Empirical Methods in Natural Language Processing*, pages 823–835.
- Fabio Petroni, Tim Rocktäschel, Sebastian Riedel, Patrick Lewis, Anton Bakhtin, Yuxiang Wu, and Alexander Miller. 2019. Language models as knowledge bases? In *Proceedings of the 2019 Conference on Empirical Methods in Natural Language Processing and the 9th International Joint Conference on Natural Language Processing (EMNLP-IJCNLP)*, pages 2463–2473.
- Ehsan Qasemi, Filip Ilievski, Muhao Chen, and Pedro Szekely. 2022. **Paco: Preconditions attributed to commonsense knowledge**.
- Alec Radford, Jong Wook Kim, Chris Hallacy, Aditya Ramesh, Gabriel Goh, Sandhini Agarwal, Girish Sastry, Amanda Askell, Pamela Mishkin, Jack Clark, et al. 2021. Learning transferable visual models from natural language supervision. In *International Conference on Machine Learning*, pages 8748–8763. PMLR.
- Colin Raffel, Noam Shazeer, Adam Roberts, Katherine Lee, Sharan Narang, Michael Matena, Yanqi Zhou, Wei Li, Peter J Liu, et al. 2020. Exploring the limits of transfer learning with a unified text-to-text transformer. *J. Mach. Learn. Res.*, 21(140):1–67.
- René Ranftl, Alexey Bochkovskiy, and Vladlen Koltun. 2021. Vision transformers for dense prediction. In *Proceedings of the IEEE/CVF International Conference on Computer Vision*, pages 12179–12188.
- Adam Roberts, Colin Raffel, and Noam Shazeer. 2020. How much knowledge can you pack into the parameters of a language model? In *Proceedings of the 2020 Conference on Empirical Methods in Natural Language Processing (EMNLP)*, pages 5418–5426.
- Shreya Shankar, Yoni Halpern, Eric Breck, James Atwood, Jimbo Wilson, and D Sculley. 2017. No classification without representation: Assessing geodiversity issues in open data sets for the developing world. *arXiv preprint arXiv:1711.08536*.
- Piyush Sharma, Nan Ding, Sebastian Goodman, and Radu Soricut. 2018. Conceptual captions: A cleaned, hypernymed, image alt-text dataset for automatic image captioning. In *Proceedings of the 56th Annual Meeting of the Association for Computational Linguistics (Volume 1: Long Papers)*, pages 2556–2565.
- Amanpreet Singh, Ronghang Hu, Vedanuj Goswami, Guillaume Couairon, Wojciech Galuba, Marcus Rohrbach, and Douwe Kiela. 2022. Flava: A foundational language and vision alignment model. In *Proceedings of the IEEE/CVF Conference on Computer Vision and Pattern Recognition*, pages 15638–15650.
- Shikhar Singh, Nuan Wen, Yu Hou, Pegah Alipoor-molabashi, Te-lin Wu, Xuezhe Ma, and Nanyun Peng. 2021. Com2sense: A commonsense reasoning benchmark with complementary sentences. In *Findings of the Association for Computational Linguistics: ACL-IJCNLP 2021*, pages 883–898.

- Robyn Speer, Joshua Chin, and Catherine Havasi. 2017. Conceptnet 5.5: An open multilingual graph of general knowledge. In *Thirty-first AAAI conference on artificial intelligence*.
- Alon Talmor, Yanai Elazar, Yoav Goldberg, and Jonathan Berant. 2020. olmpics-on what language model pre-training captures. *Transactions of the Association for Computational Linguistics*, 8:743–758.
- Alon Talmor, Jonathan Herzig, Nicholas Lourie, and Jonathan Berant. 2019. Commonsenseqa: A question answering challenge targeting commonsense knowledge. In *Proceedings of the 2019 Conference of the North American Chapter of the Association for Computational Linguistics: Human Language Technologies, Volume 1 (Long and Short Papers)*, pages 4149–4158.
- Endel Tulving. 1972. *Episodic and semantic memory*. Organization of memory., pages xiii, 423–xiii, 423. Academic Press, Oxford, England.
- Alex Wang, Yada Pruksachatkun, Nikita Nangia, Amanpreet Singh, Julian Michael, Felix Hill, Omer Levy, and Samuel Bowman. 2019. Superglue: A stickier benchmark for general-purpose language understanding systems. *Advances in neural information processing systems*, 32.
- Peng Wang, An Yang, Rui Men, Junyang Lin, Shuai Bai, Zhikang Li, Jianxin Ma, Chang Zhou, Jingren Zhou, and Hongxia Yang. 2022. Ofa: Unifying architectures, tasks, and modalities through a simple sequence-to-sequence learning framework. In *International Conference on Machine Learning*, pages 23318–23340. PMLR.
- Jianwei Yang, Chunyuan Li, Pengchuan Zhang, Bin Xiao, Ce Liu, Lu Yuan, and Jianfeng Gao. 2022. Unified contrastive learning in image-text-label space. In *Proceedings of the IEEE/CVF Conference on Computer Vision and Pattern Recognition*, pages 19163–19173.
- Da Yin, Hritik Bansal, Masoud Monajatipoor, Liunian Harold Li, and Kai-Wei Chang. 2022. Geomlana: Geo-diverse commonsense probing on multilingual pre-trained language models. *arXiv preprint arXiv:2205.12247*.
- Da Yin, Liunian Harold Li, Ziniu Hu, Nanyun Peng, and Kai-Wei Chang. 2021. Broaden the vision: Geo-diverse visual commonsense reasoning. In *Proceedings of the 2021 Conference on Empirical Methods in Natural Language Processing*, pages 2115–2129.
- Rowan Zellers, Yonatan Bisk, Ali Farhadi, and Yejin Choi. 2019. From recognition to cognition: Visual commonsense reasoning. In *Proceedings of the IEEE/CVF conference on computer vision and pattern recognition*, pages 6720–6731.
- Bolei Zhou, Hang Zhao, Xavier Puig, Sanja Fidler, Adela Barriuso, and Antonio Torralba. 2017. Scene parsing through ade20k dataset. In *Proceedings of the IEEE conference on computer vision and pattern recognition*, pages 633–641.
- Zhengxia Zou, Zhenwei Shi, Yuhong Guo, and Jieping Ye. 2019. Object detection in 20 years: A survey. *arXiv preprint arXiv:1905.05055*.

Appendix

A Implementation Details

A.1 Pipeline Parameters

To cluster objects for computing relative size, we use Jenks Natural Breaks (Jenks, 1967), with $\#clusters = 5$ following the manual groupings of object sizes in Liu et al. (2022b). We also experimented with $\#clusters = 3$, but qualitatively observed less optimal clusters. In spatial module, we create 3 partitions of uniform size and overlap.

A.2 Typical Labels

We derive typical labels from the raw label probabilities (C) by filtering classes as per a predefined threshold p_{min} , that can be interpreted as either noise or rare occurrence. Formally, we apply the filter as follows: $C = \{(c, p) | p > p_{min}, (c, p) \in C\}$. Here, p_{min} is defined as:

$$\begin{cases} 10\% & 4 \leq |C| \leq 11 \\ 20\% & |C| = 3 \\ 30\% & |C| = 2 \end{cases}$$

The resulting distribution is re-normalized and the filtering step is applied recursively.

A.3 Defining Spatial Relations

Our objective is to map the raw coordinates in an image for two objects to discrete relations. We define a simple set of rules to convey *above* and *similar* level, from object annotations. Given bounding box or polygon mask, we first compute its centroid along with the lowest point. We then compare the y-coordinates of objects as illustrated in Fig. 6. If an object’s lowest point is above the other’s centroid, we map it to *above*, else *similar* level.

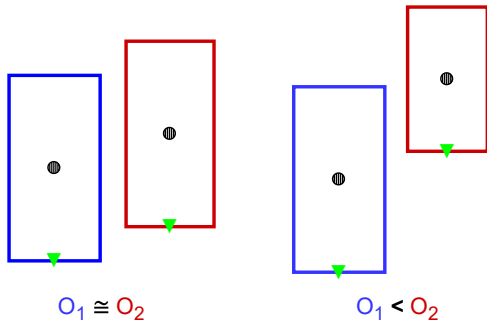


Figure 6: Illustrates our definition of spatial relation from raw annotations.

A.4 Prediction to Basic Color

We use OFA in our pipeline, and map generated text to the basic color set as shown in Table 7. If the model predicts multiple colors, we assign each of them to the object instance.

Basic Color	Raw Predicted Terms
Yellow	<i>gold, golden, blonde, beige, peach, cream</i>
Brown	<i>wooden, tan, beige, bronze, copper</i>
Gray	<i>grey, silver, metal, steel</i>
Pink	<i>peach</i>
Purple	<i>violet</i>
Red	<i>maroon</i>
Green	<i>teal</i>
Blue	<i>teal, turquoise</i>

Table 7: Mapping between raw predictions (OFA) and basic color terms.

Context	Examples
Event	<i>wedding cake, bathing soap</i>
Location	<i>kitchen sink, street lamp</i>
State	<i>bare tree, sliced apple</i>
Part	<i>piano key, bike wheel</i>

Table 8: Context-based subtype examples

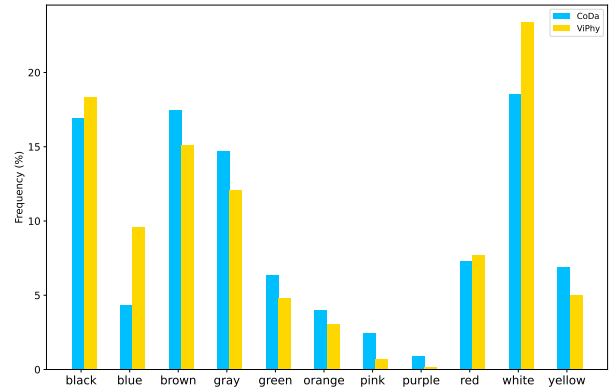


Figure 7: Color distribution of objects in VIPHY and CoDa.

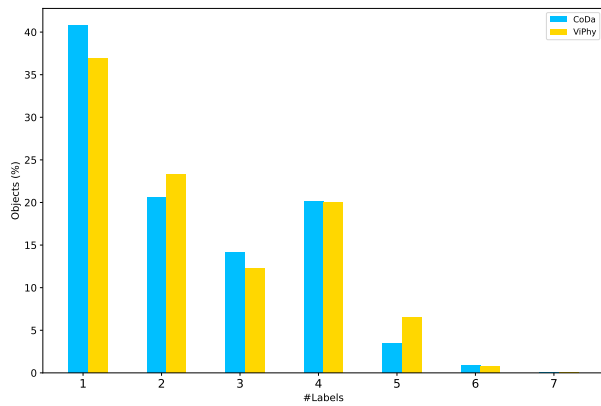


Figure 8: Color distribution with respect to label cardinality in ViPHY and CoDa.



Figure 9: A sample image and corresponding captions from Visual Genome dataset. Illustrates how humans omit the subtype *kitchen sink*, when annotating images.

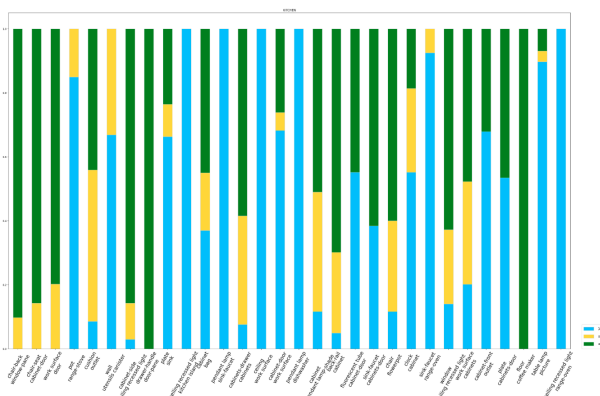


Figure 10: Spatial relation distribution for object pairs in *kitchen* scene from ViPHY.

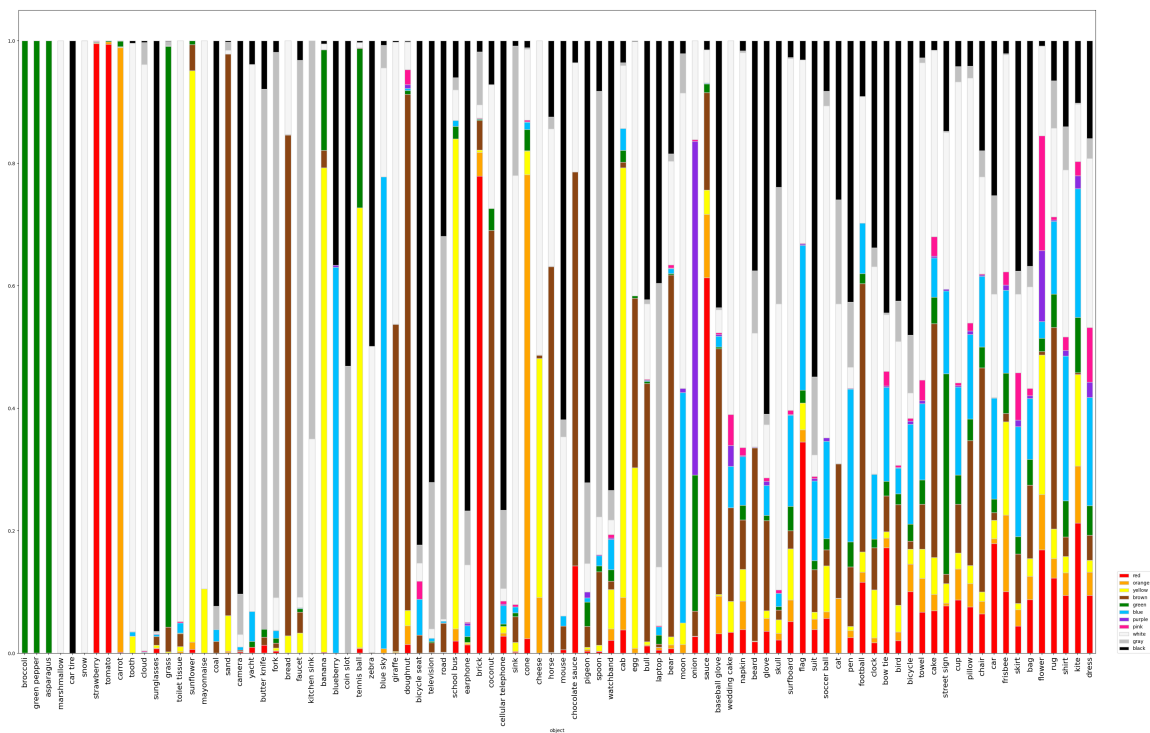


Figure 11: Color distribution for 90 objects from VIPHY, sorted by entropy.